



# Research on $\text{YAl}_2$ intermetallics particles reinforced Mg–14Li–3Al matrix composites

G.Q. Wu\*, Z.H. Ling, X. Zhang, S.J. Wang, T. Zhang, Z. Huang

School of Materials Science and Engineering, Beihang University, 37 Xueyuan Road, Beijing 100191, PR China

## ARTICLE INFO

### Article history:

Received 1 November 2009

Received in revised form 19 July 2010

Accepted 20 July 2010

Available online 29 July 2010

### Keywords:

Mg–Li alloy

Composite

Intermetallics

Mechanical property

Interface

Finite element modeling

## ABSTRACT

A novel Mg–14Li–3Al (LA143) matrix composite reinforced with  $\text{YAl}_2$  intermetallics particles was developed by stir-casting. The microstructure and interface characteristics of the  $\text{YAl}_{2p}$ /LA143 composite were investigated. The results show that,  $\text{YAl}_2$  particles distribute uniformly in the composite, and a good interfacial bonding is obtained with no reaction products at particle/matrix interfaces.  $\text{YAl}_{2p}$ /LA143 composite exhibits excellent mechanical properties. The tensile strength and yield strength are significantly improved by the addition of  $\text{YAl}_2$  particles, while a good ductility property is kept. During tensile deformation,  $\text{YAl}_2$  particles may prevent the propagation of crack in microscale. The  $\text{YAl}_2$  particles can be compatible with the deformation of the matrix due to their deformation, exhibiting a “soft” restriction to the matrix. Therefore, the strength and toughness of the  $\text{YAl}_{2p}$ /LA143 composite can be improved by the above effects.

Crown Copyright © 2010 Published by Elsevier B.V. All rights reserved.

## 1. Introduction

Mg–Li based alloys, known as the lightest metallic structural materials, have been widely studied both theoretically and experimentally [1–3]. Due to their attractive features of high values of specific strength and specific modulus, excellent anti-shock and electromagnetic shielding properties, Mg–Li based alloys have great potential for use not only in aerospace and military but also in automobiles and electrical appliances [4,5]. However, Mg–Li based alloys have intrinsic problems such as aging stability, low tensile strength and poor corrosion resistance [6,7]. These problems would limit their widespread applications. To improve the strength of Mg–Li based alloys, various elements have been added [7,8]. But, these alloys show strength degradation due to ageing and poor corrosion resistance. The composite strengthening is one of the feasible ways to improve the strength and to prevent the degradation of mechanical properties of Mg–Li based alloys [9].  $\text{SiC}$ ,  $\text{Al}_2\text{O}_3$  fibers and  $\text{Mg}_2\text{Si}$  particles [10–12] have been used to reinforce Mg–Li based alloys recently. The results [12] show that the ceramic reinforcements can substantially improve the mechanical properties of Mg–Li based alloys. However, the chemical incompatibility between ceramic reinforcements and Mg–Li alloy matrix remains a critical problem to be solved, which is harmful to the ductility of the composites. Thus, some intermetallic compounds

that own relatively high specific strength as well as high specific stiffness and have good chemical compatibility with metals or alloys, have been selected and utilized as the promising reinforcements of metal matrix composites [13–15]. Compared with Mg–Li based alloys,  $\text{YAl}_2$  intermetallic compound has high melting temperature (1748 K), high Young's modulus (158 GPa), high hardness ( $\text{HV} = 645$ ) and relatively low coefficient of thermal expansion ( $\text{CTE} = 10 \times 10^{-6} \text{ K}^{-1}$ ). So it can be supposed that  $\text{YAl}_2$  particle reinforcement Mg–Li based composites possess favorable properties.

In this paper,  $\text{YAl}_2$  particles were chosen as reinforcement to prepare Mg–14Li–3Al matrix composite, and the microstructure, interface characteristics, mechanical properties and fracture behavior were investigated systematically.

## 2. Materials and methods

In this study, Mg–14Li–3Al (LA143) alloy was used as matrix alloy, and  $\text{YAl}_2$  intermetallics particles (obtained from General Research Institute for Nonferrous Metals) with an average size smaller than  $37.5 \mu\text{m}$  were chosen as reinforcement. Mg–14Li–3Al (LA143) alloy and the 20 vol%  $\text{YAl}_{2p}$ /LA143 composite were prepared by stir-casting at  $650^\circ\text{C}$  in a resistance furnace under an argon atmosphere. The superheated slurry was stirred at 720 r/min for 30 min.

The microstructures and structures of the composite were characterized by XJP-3C optical microscope (OM), JSM-5800 scanning electron microscope (SEM) and D/MAX-2000 X-ray diffractometer (XRD). Interface characteristics of  $\text{YAl}_{2p}$ /LA143 composite were carried out using Hitachi H-800 transmission electron microscopy (TEM) and JEM-2100F high-resolution electron microscopy (HREM), operating at 200 kV.

The room-temperature and high-temperature mechanical properties were examined by MTS-880 material testing machine at a strain rate of 0.5 mm/min rate. The subsize flat specimens (12.5 mm in gauge length, 4 mm in width, and 3 mm in

\* Corresponding author. Tel.: +86 1082313240; fax: +86 1082313240.

E-mail address: [guoqingwu@buaa.edu.cn](mailto:guoqingwu@buaa.edu.cn) (G.Q. Wu).

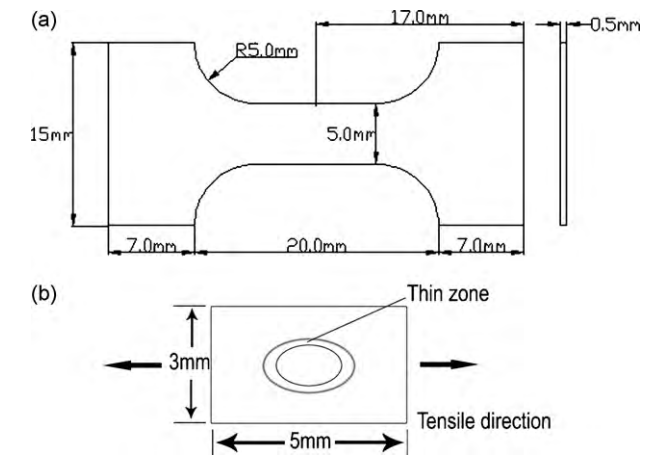


**Fig. 1.** Configurations of the tensile specimens for SEM/TEM in situ observation. (a) SEM, (b) TEM.

**Table 1**  
The parameters of materials for simulation.

Materials	Elastic modulus (GPa)	Tensile strength (MPa)	Poisson's ratio
Matrix	34.5	120	0.31
Reinforcement	100/300/500	800	0.25

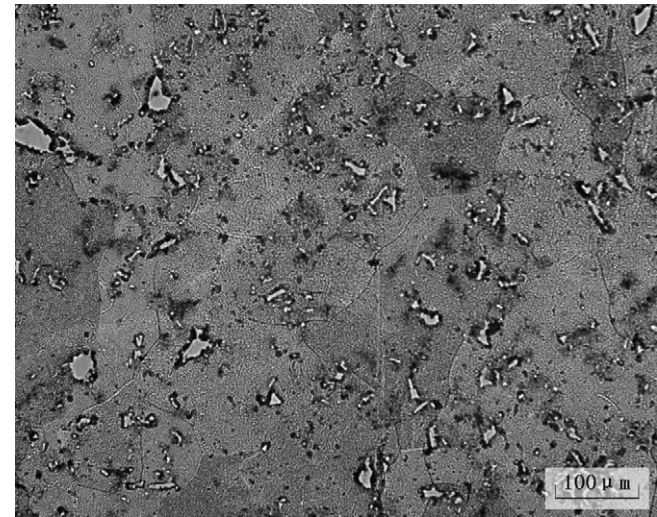


**Fig. 2.** OM microstructure of the as-cast YAl<sub>2</sub>p/LA143 composite.

thickness) were machined from the central region of the ingots. An MTS 632.12C-20 extensometer with 25 mm gauge length (+12.5 mm/−2.5 mm range) was used to measure yield strength, tensile strength and elongation.

In situ tensile test of the composite was used to observe fracture and deformation processes by JSM-5800 scanning electron microscope (SEM) and Hitachi H-800 transmission electron microscope (TEM), respectively. The configurations of in situ tensile specimens are shown in Fig. 1. A notch of 0.25 mm in width and 80 μm in root radius was cut perpendicular to the loading direction in the middle of specimen for SEM in situ observation using electrical discharge machining (EDM).

**Table 2**  
Tensile properties of the monolithic matrix alloy and composite.

Materials	Temperature	$\sigma_b$ (MPa)	$\sigma_{0.2}$ (MPa)	$\varepsilon$ (%)	$E$ (GPa)	$\rho$ (g/cm <sup>3</sup> )
Mg–14Li–3Al (LA143)	20 °C	115	94	26	34.5	1.36
20 vol%YAl <sub>2</sub> p/LA143	20 °C	225	161	9	73.2	1.52
Mg–14Li–3Al (LA143)	180 °C	37	20	34	–	1.36
20 vol%YAl <sub>2</sub> p/LA143	180 °C	78	57	18	–	1.52

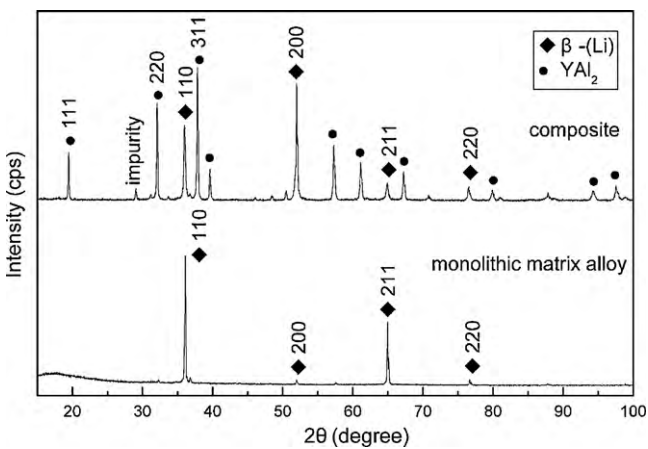


**Fig. 3.** X-ray diffraction patterns of monolithic matrix alloy and composite.

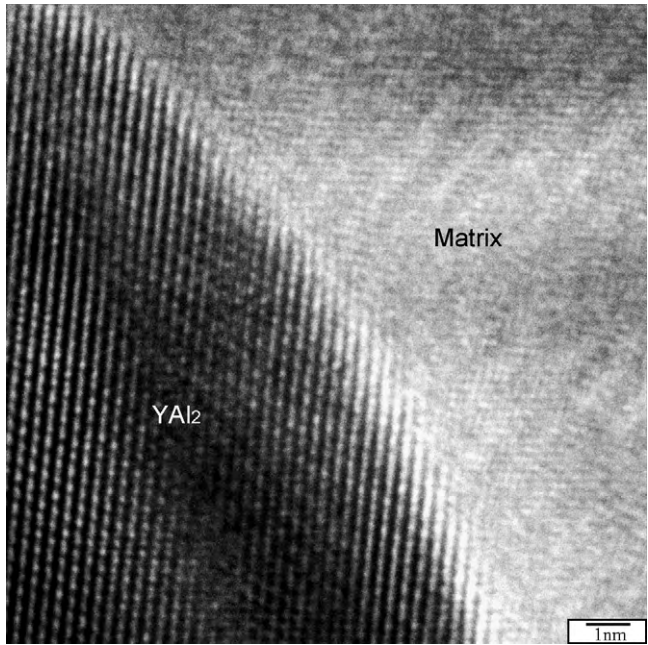


**Fig. 4.** HREM micrograph of the interface between YAl<sub>2</sub> particle and matrix.

The tensile deformation behavior and features of the composite were simulated by finite element method. The parameters of material for simulation are shown in Table 1.

**3. Results and discussion**

**3.1. Microstructure and interface characteristics**

The microstructure of as-cast YAl<sub>2</sub>p/LA143 composite is shown in Fig. 2. The YAl<sub>2</sub> particles distribute homogenously in the grains and grain boundaries of the matrix, while no obvious particles agglomeration phenomenon is observed. X-ray diffraction patterns (Fig. 3) indicate that the composite consists of β-(Li) phase and YAl<sub>2</sub>



phase. A few small peaks (marked as impurity) in the XRD patterns of the composite could not be identified. The impurity was introduced by the raw  $\text{YAl}_2$  intermetallic particles, not a product of the composite. Besides, with the addition of  $\text{YAl}_2$  particles, the grain size of the composite (about  $150\text{ }\mu\text{m}$ ) was decreased to  $1/3$  of the original grain of the matrix alloy (approximately  $550\text{ }\mu\text{m}$ ).

The interface characteristics between  $\text{YAl}_2$  particle and LA143 alloy matrix were observed and analyzed by transmission electron microscopy (TEM) and high-resolution electron microscopy (HREM). The HREM image (Fig. 4) indicates that  $\text{YAl}_2$  particle bonds well with LA143 matrix without forming an intermediate phase. And there are no porosities or reaction products found in the interface. The interface is clean, strongly bonded and has a good continuity. The  $\text{YAl}_2$  particles are stable in LA143 alloy matrix. The stability of  $\text{YAl}_2$  intermetallics in the  $\beta$ -(Li) phase, as observed above, would be of great significance in obtaining excellent comprehensive mechanical properties of  $\text{YAl}_{2p}$ /LA143 composite.

### 3.2. Mechanical properties and fracture behavior

The tensile properties of  $\text{YAl}_{2p}$ /LA143 composite both at room temperature and high temperature are shown in Table 2. The addition of  $\text{YAl}_2$  intermetallics particles can effectively improve the room temperature mechanical properties of the matrix alloy. The yield strength, tensile strength, Young's modulus, density-specific strength of the composite are 161 MPa, 225 MPa, 73.2 GPa and  $148\text{ MPa/g/cm}^3$ , respectively, which increased by 71.3%, 95.6%, 112.2% and 74.1% as compared with the matrix alloy. Meanwhile, the elongation remains at 9%, indicating that the ductility property of the composite is well kept. In a certain temperature range,

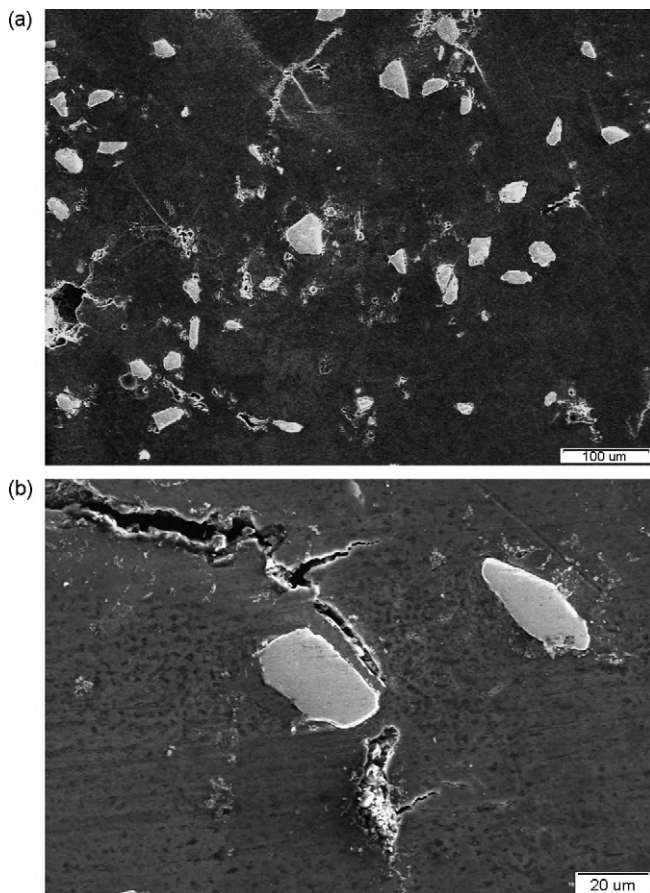


**Fig. 5.** SEM in situ observation of the initiation and propagation of the cracks. (a) Initiation of the cracks, (b) propagation of the cracks.

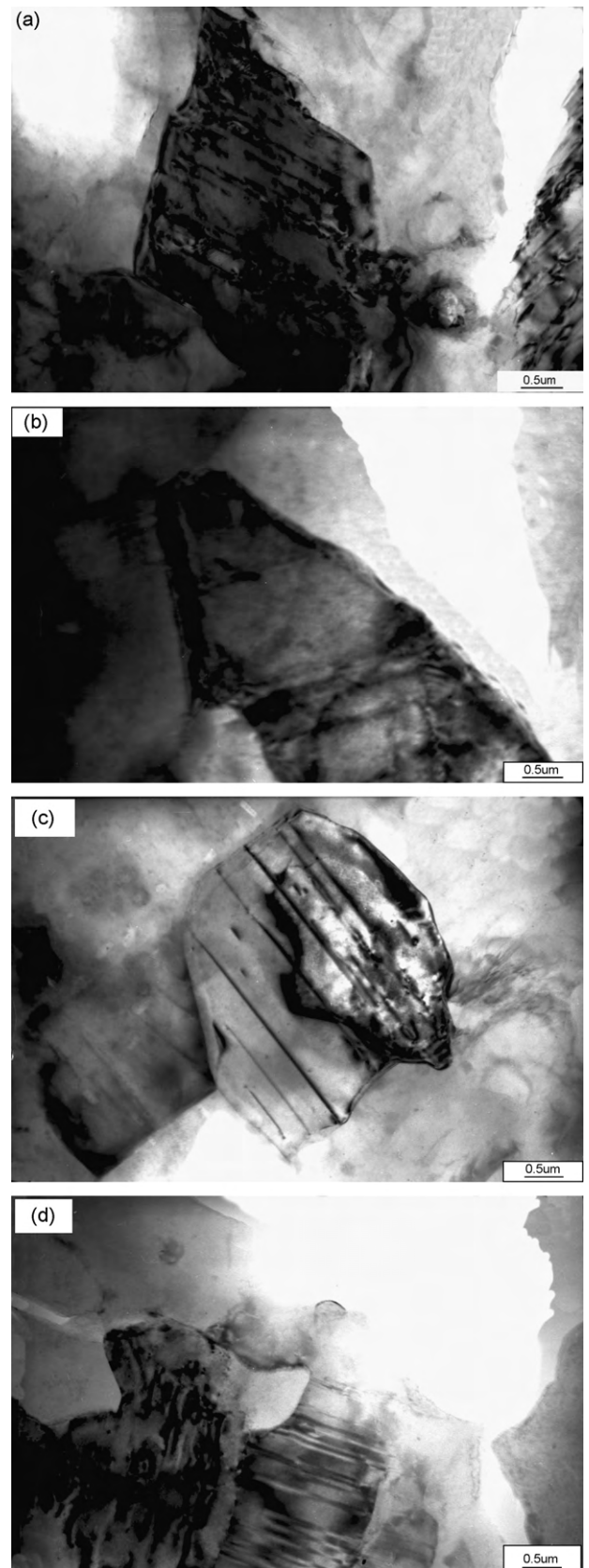


**Fig. 6.** Interaction between twin and  $\text{YAl}_2$  particles. (a) and (b) initiation of twin, (c) and (d) propagation of twin.

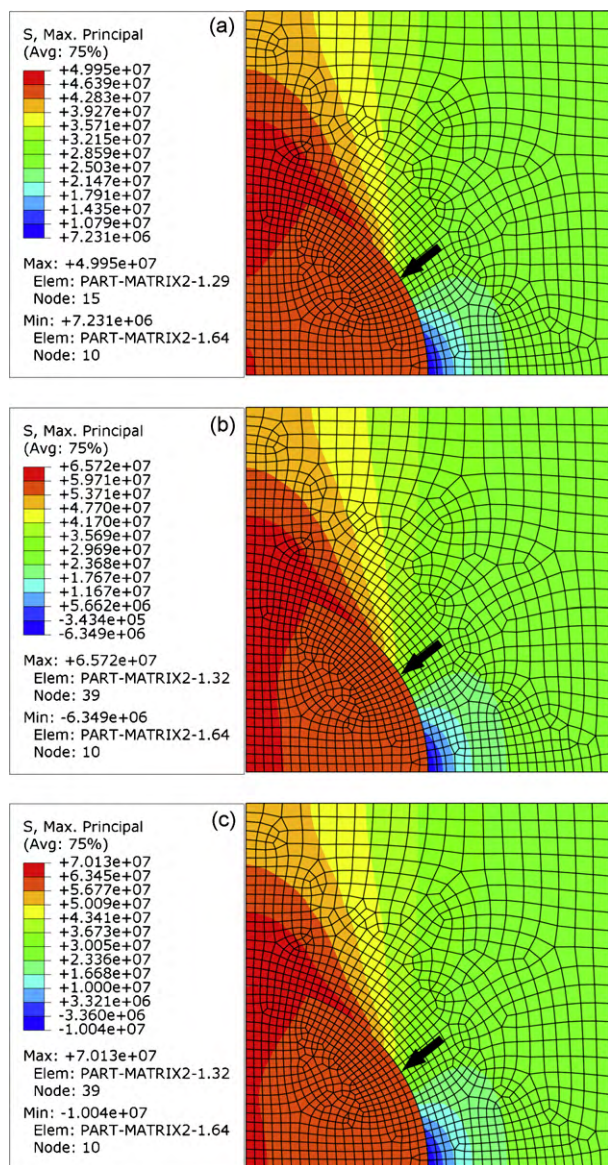


Fig. 7. Principal stress distributions of the composites with different particle's elastic modulus. (a)  $E = 100$  GPa, (b)  $E = 300$  GPa, (c)  $E = 500$  GPa.

the high-temperature deformation resistance of the composite has been greatly enhanced due to the addition of  $\text{YAl}_2$  intermetallics. The pinning effect of particles in the composite hinders the movement of dislocations and the operation of slip systems. At  $180^\circ\text{C}$ , the tensile strength, yield strength and density-specific strength of 20 vol% $\text{YAl}_2$ /LA143 composite are 78 MPa, 57 MPa and 51 MPa/g/cm<sup>3</sup>, respectively, which increased by 110%, 185% and 88.9% as compared with the matrix alloy.

The in situ observation of fracture process in composite by SEM implies that the micro-cracks mainly initiate in the matrix (Fig. 5(a)) rather than in the interfaces, and the micro-cracks propagate in the matrix that is close to the interface (Fig. 5(b)). The  $\text{YAl}_2$  particles are more “soft” as compared with ceramics. The in situ observation of deformation process in composite by TEM implies that  $\text{YAl}_2$  particles can be compatible with the deformation of the matrix due to their deformation (Fig. 6), exhibiting a “soft” restriction to the matrix. Besides, the  $\text{YAl}_2$  particles may resist the propagation of cracks in micro-scale during deformation of the composite.

### 3.3. Finite element modelling of tensile deformation

To further study the effects of  $\text{YAl}_2$  particles on strength and toughness of composite, a finite element model was built to simulate the local stress field of the particles with different elastic modulus. The influences of reinforcements with various strength and modulus on the micromechanics characteristics of composites are investigated. Fig. 7 shows the principal stress distributions of composites with different particle's elastic modulus during elastic deformation. The edge of the reinforcement particles is marked by arrows. Due to the differences in the elastic modulus between reinforcements and matrix, the reinforcements will impose strain restriction on the matrix which is close to the interface and transform some local regions to the high-stress areas. Meanwhile, the stresses around the reinforcements will be partly released and form some low-stress areas at the edge of particles. Thus, the so-called interface mechanics transition layer [16] is finally formed. When particle's elastic modulus is relatively low (Fig. 7(a)), the reinforcement imposes small strain restriction on matrix, and then the stresses of composite will be well-distributed, the reinforcement particles exhibiting a “soft” restriction to the matrix. As the particle's elastic modulus getting higher (Fig. 7(b) and (c)), the stress of reinforcement is getting higher too, which indicates its load-sharing function is enhanced gradually. Meanwhile, the strain restriction that reinforcement imposed on the matrix becomes larger, which causes the maximum stress of composite to increase gradually. As a result, stress concentration forms in some areas of the composite. The micro-cracks will initiate easily in these stress concentration areas during tensile deformation of the materials.

The above simulation results are consistent with the results of dynamic tensile test. Using relatively “hard” ceramic particles with high modulus and strength to reinforce the metal matrix, a large number of micro-cracks can be observed in the particles and interfaces during tensile deformation. Conversely, using relatively “soft” intermetallics particles with relatively low modulus and strength to reinforce the metal matrix, not only the tendency of crack initiation in the particles and interfaces can be alleviated, but also the propagation of crack may be restricted by particles. The application of  $\text{YAl}_2$  intermetallics particles will be benefit to alleviate damages to the plasticity and toughness of matrix alloy caused by reinforcement.

## 4. Conclusions

The primary conclusions that may be derived from this work are as follows:

- (1) The  $\text{YAl}_2$ /LA143 composite consists of  $\beta$ -(Li) phase and  $\text{YAl}_2$  phase. The  $\text{YAl}_2$  particles distribute homogeneously in the grains and grain boundaries of the matrix. The addition of  $\text{YAl}_2$  particles can refine grains of the matrix alloy. The interfaces between  $\text{YAl}_2$  particles and LA143 alloy matrix bond well. There are no interfacial cracking, porosities and transition layers found in micro-scale.
- (2) The mechanical properties of  $\text{YAl}_2$ /LA143 composite are significantly improved compared with matrix alloy, while a good ductility property is kept. At room temperature, the tensile strength, yield strength, Young's modulus and elongation of 20 vol% $\text{YAl}_2$ /LA143 composite are 225 MPa, 161 MPa, 73.2 GPa and 9% respectively.
- (3) The addition of  $\text{YAl}_2$  intermetallics particles can also improve the deformation resistance of matrix alloy at high temperature. At  $180^\circ\text{C}$ , the tensile strength and yield strength of 20 vol% $\text{YAl}_2$ /LA143 composite are 78 MPa and 57 MPa, respec-

tively, which increased by 110% and 185% as compared with matrix alloy.

- (4) The cracks mainly initiate in the matrix, and propagate in the matrix which is close to the particle/matrix interfaces during tensile deformation process of the composite. The  $\text{YAl}_2$  particles may resist the propagation of crack in micro-scale. They can be compatible with matrix due to their deformation, exhibiting a “soft” restriction to the matrix. Thus, the LA143 alloy reinforced by  $\text{YAl}_2$  intermetallics particles can remain at a high strength and toughness simultaneously.

### Acknowledgements

The work was financially supported by the Ph.D. Programs Foundation of Ministry of Education of China (20070006020) and the Beijing Nova Program (2007B016).

### References

- [1] W.A. Counts, M. Friák, D. Raabe, J. Neugebauer, *Acta Mater.* 57 (2009) 69–76.
- [2] C.P. Liang, H.R. Gong, *J. Alloys Compd.* 489 (2010) 130–135.
- [3] T. Al-Samman, *Acta Mater.* 57 (2009) 2242–2299.
- [4] T. Liu, S.D. Wu, S.X. Li, P.J. Li, *Mater. Sci. Eng. A* 460–461 (2007) 499–503.
- [5] W.J. Kim, M.J. Kim, J.Y. Wang, *Mater. Sci. Eng. A* 516 (2009) 17–22.
- [6] L.H. Yang, J.Q. Li, Y.Z. Zheng, W.W. Jiang, M.L. Zhang, *J. Alloys Compd.* 467 (2009) 562–566.
- [7] H.Y. Wu, Z.W. Gao, J.Y. Lin, C.H. Chiu, *J. Alloys Compd.* 474 (2009) 158–163.
- [8] X.R. Meng, R.Z. Wu, M.L. Zhang, L.B. Wu, C.L. Cui, *J. Alloys Compd.* 486 (2009) 722–725.
- [9] S. Kúdela, *Int. J. Mater. Prod. Technol.* 18 (2003) 91–115.
- [10] H.S. Yu, R.L. Gao, G.H. Min, Z.F. Wang, X.C. Chen, *Trans. Nonferrous Met. Soc. China* 12 (2002) 1154–1157.
- [11] S. Kúdela Jr., H. Wendrock, S. Kúdela, A. Pawełek, A. Piątkowski, K. Wetzig, *Int. J. Mater. Res.* 100 (2009) 910–914.
- [12] Z. Trojanová, Z. Drozd, S. Kúdela, Z. Száraz, P. Lukáč, *Compos. Sci. Technol.* 67 (2007) 1965–1973.
- [13] V. Abbasi Chianeha, H.R. Madaah Hosseini, M. Nofar, *J. Alloys Compd.* 473 (2009) 127–132.
- [14] H.A. Pour, M. Lieblch, A.J. López, J. Rams, M.T. Salehi, S.G. Shabestari, *Compos. Part A: Appl. Sci. Manuf.* 38 (2007) 2536–2540.
- [15] G. Laplanche, A. Joulain, J. Bonneville, R. Schaller, T. El Kabir, *J. Alloys Compd.* 493 (2010) 453–460.
- [16] X.J. Li, D.L. Chai, Y.L. Xi, *Acta Metall. Sin. (China)* 40 (2004) 927–929.